

# Nuclear modification factor in an anisotropic *Quark-Gluon-Plasma*

Mahatsab Mandal<sup>a</sup> Lusaka Bhattacharya<sup>b</sup> and Pradip Roy<sup>c</sup>

*Saha Institute of Nuclear Physics*

*1/AF Bidhannagar, Kolkata - 700064, INDIA*

## ABSTRACT

We calculate the nuclear modification factor ( $R_{AA}$ ) of light hadrons by taking into account the initial state momentum anisotropy of the quark gluon plasma (QGP) expected to be formed in relativistic heavy ion collisions. Such an anisotropy can result from the initial rapid longitudinal expansion of the matter. A phenomenological model for the space time evolution of the anisotropic QGP is used to obtain the time dependence of the anisotropy parameter  $\xi$  and the hard momentum scale,  $p_{\text{hard}}$ . The result is then compared with the PHENIX experimental data to constrain the isotropization time scale,  $\tau_{\text{iso}}$  for fixed initial conditions (FIC). It is shown that the extracted value of  $\tau_{\text{iso}}$  lies in the range  $0.5 \leq \tau_{\text{iso}} \leq 1.5$ . However, using fixed final multiplicity (FFM) condition does not lead to any firm conclusion about the extraction of the isotropization time. The present calculation is also extended to contrast with the recent measurement of nuclear modification factor by ALICE collaboration at  $\sqrt{s} = 2.76$  TeV. It is argued that in the present approach, the extraction of  $\tau_{\text{iso}}$  at this energy is uncertain and, therefore, refinement of the model is necessary. The sensitivity of the results on the initial conditions has been discussed. We also present the nuclear modification factor at LHC energies with  $\sqrt{s} = 5.5$  TeV.

## 1 Introduction

The partonic energy loss in a QCD plasma has received significant attention in recent years. Experimentally, the partonic energy loss can be probed by measuring the high  $p_T$  hadrons emanating from ultra-relativistic heavy ion collisions. This idea was first proposed by Bjorken [1] where ‘ionization loss’ of the quarks and gluons in a QCD plasma was estimated. In fact, the ‘stopping power’ ( $dE/dx$ ) of the plasma is proportional to  $\sqrt{\epsilon}$ , where,  $\epsilon$  is the energy density of the partonic medium. Therefore, by measuring various high  $p_T$  observables one can probe the initial parton density [1].

Hard partons, injected into hot QCD medium, can dissipate energy in two ways, *viz.*, by two body collisions or *via* the bremsstrahlung emission of gluons, commonly referred to

---

<sup>a</sup>E-mail address: mahatsab.mandal@saha.ac.in

<sup>b</sup>E-mail address: lusaka.bhattacharya@saha.ac.in

<sup>c</sup>E-mail address: pradipk.roy@saha.ac.in

as collisional and radiative loss respectively. For electromagnetic processes, it is well known that at large energies, radiative losses are much higher than the collisional loss.

The possibility of QGP formation at RHIC experiment, with initial density of  $5 \text{ GeV}/fm^3$  is supported by the observation of high  $p_T$  hadron suppression (jet-quenching) in the central Au-Au collisions compared to the binary-scaled hadron-hadron collisions [2]. The phenomena of jet-quenching has been investigated by various authors [2]. Apart from jet-quenching, several possible probes have been studied in order to characterize the properties of QGP.

However, many properties of QGP are still poorly understood. The most debated question is whether the matter formed in the relativistic heavy ion collisions is in thermal equilibrium or not. The measurement of elliptic flow parameter and its theoretical explanation suggest that the matter quickly comes into thermal equilibrium (with  $\tau_{\text{therm}} < 1 \text{ fm}/c$ , where  $\tau_{\text{therm}}$  is the time of thermalization) [3]. As for example, one of the major difficulty is to measure the thermalization ( $\tau_{\text{therm}}$ ) and isotropization ( $\tau_{\text{iso}}$ ) time of the QGP. On the one hand, the success of ideal hydrodynamic fits to experimental data [3] implies rapid thermalization of the bulk matter created at RHIC. On the contrary, perturbative estimation suggests relatively slower thermalization of QGP [4]. However, recent hydrodynamical studies [5] have shown that due to the poor knowledge of the initial conditions there is a sizable amount of uncertainty in the estimate of thermalization or isotropization time. It is suggested that (momentum) anisotropy driven plasma instabilities may speed up the process of isotropization [6], in that case one is allowed to use hydrodynamics for the evolution of the matter. However, instability-driven isotropization is not yet proved at RHIC and LHC energies.

In absence of a theoretical proof favoring the rapid thermalization and the uncertainties in the hydrodynamical fits of experimental data, it is very hard to assume hydrodynamical behavior of the system from the very beginning. Therefore, it has been suggested to look for some observables which are sensitive to the early time after the collision. For example, jet-quenching vis-a-vis energy loss of partons could be an observable where the initial state momentum anisotropy can play important role. It is to be noted that the calculations of energy loss in Ref. [2] have been performed in isotropic QGP which is true immediately after its formation [7]. However, subsequent rapid expansion of the matter along the beam direction causes faster cooling in the longitudinal direction than in the transverse direction [4]. As a result, the system becomes anisotropic with  $\langle p_L^2 \rangle \ll \langle p_T^2 \rangle$  in the local rest frame. At some later time when the effect of parton interaction rate overcomes the plasma expansion rate, the system returns to the isotropic state again and remains isotropic for the rest of the period. Thus, during the early stage the plasma remains anisotropic and any calculation of energy loss should, in principle, include this aspect. The collisional energy loss in anisotropic media for heavy fermions has been calculated in Refs. [8, 9]. In these calculations it is found that the deviations from the isotropic results are of the order of 10% for  $\xi = 1$  ( $\xi$  is the anisotropy parameter) and of the order of 20% for  $\xi = 10$ . It is observed that the collisional energy loss varies with the angle of propagation by upto 50%.

Radiative energy loss in anisotropic QGP has recently been calculated in Ref. [10] in first order opacity expansion where the scatterers are treated as static. It should be noted that the energy loss of a parton in anisotropic media depends both on the anisotropy parameter and the direction of propagation with respect to the anisotropy axis  $\hat{n}$ . In that case, general expression for the two-body potential should be used [10]. Few comments about the calculation of radiative energy loss are in order here. First of all we have considered scattering

from static charges in which case only longitudinal gauge bosons are exchanged rendering the screened potential stable. The effect of anisotropy would be significantly different if one considers the recoil of the scattering centre. In case of moving scatterer, transverse (magnetic) gluon exchange results plasma instabilities which has to be taken into account. It is worthwhile to mention that the growth of unstable modes in anisotropic media greatly influences the transport co-efficients and hence the energy loss. This is recently demonstrated in Ref. [11]. Considering a two-stream plasma the authors in [11] show that the momentum broadening grows exponentially with time as the spontaneously growing fields exert an exponentially growing influence on the propagating parton. In an evolving plasma this aspect is an important component without which the results remain somewhat like a zeroth order approximation. However, in the present work, we do not include this effect and assume that the fragmenting partons propagate in the direction of anisotropy.

For a parton propagating in the direction of anisotropy it is found that the fractional energy loss increases by a factor of 1.5 - 2 depending upon the anisotropy parameter  $\xi$ . In the present work, we shall apply this formalism to calculate the nuclear modification factor for light hadrons. A phenomenological model for the space-time evolution will be used for the time evolution of  $\xi$  and  $p_{\text{hard}}$ . Since the role of collisional energy loss in the context of RHIC data is not settled yet, we shall not include this process in the present work.

The plan of the paper is the following. In section 2 we briefly recall the necessary ingredients to calculate radiative energy loss in anisotropic media. Then we discuss how this can be implemented to calculate  $R_{\text{AA}}$  along with space-time model for anisotropic media. Section 3 will be devoted to discuss the results. Finally, we conclude in section 4.

## 2 Formalism

### 2.1 Radiative energy loss

In this section, we briefly mention the formalism of the radiative energy loss in an infinitely extended anisotropic plasma (see Ref. [10] for further details).

We assume that an on-shell quark produced in the remote past is propagating through an infinite QCD medium that consists of randomly distributed static scattering centers which provides a color-screened Yukawa potential originally developed for the isotropic QCD medium given by [12]

$$\begin{aligned} V_n &= V(q_n) e^{i\vec{q}_n \cdot \vec{x}_n} \\ &= 2\pi\delta(q^0) v(q_n) e^{-i\vec{q}_n \cdot \vec{x}_n} T_{a_n}(R) \otimes T_{a_n}(n). \end{aligned} \quad (1)$$

with  $v(\vec{q}_n) = 4\pi\alpha_s/(\vec{q}_n^2 + \mu^2)$ , where  $\mu$  is the Debye mass.  $x_n$  is the location of the  $n$ th scattering centre,  $T$  (summed over  $a_n$ ) denotes the colour matrices of the parton and the scattering centre. It is to be noted that the potential has been derived by using hard thermal loop (HTL) propagator in QGP medium. In a plasma with momentum anisotropy the two body interaction, as expected, becomes direction dependent. In addition, it depends on the anisotropy parameter  $\xi$  and the hard momentum scale  $p_{\text{hard}}$  in the following way:

$$f(\vec{p}) = \frac{1}{e^{p/p_{\text{hard}}} \sqrt{1+\xi(\vec{p} \cdot \vec{n})^2} \pm 1} \quad (2)$$

where, the parameter  $\xi$  is the degree of anisotropy parameter ( $-1 < \xi < \infty$ ) and is given by  $\xi = \langle p_T^2 \rangle / (2 \langle p_z^2 \rangle) - 1$ . It is to be noted that  $\xi$  can also be related to the shear viscosity [13].

To calculate the two body potential appearing in Eq.(1) one starts with the retarded gluon self energy expressed as [14]

$$\Pi^{\mu\nu}(P) = g^2 \int \frac{d^3k}{(2\pi)^3} v^\mu \frac{\partial f(\vec{k})}{\partial K^\beta} \left( g^{\nu\beta} - \frac{v^\nu P^\beta}{P \cdot v + i\epsilon} \right) \quad (3)$$

We have adopted the following notation for four vectors:  $P^\mu = (p_0, \vec{p}) = (p_0, \mathbf{p}, p_z)$ , i. e.  $\vec{p}$  (with an explicit vector superscript) describes a three-vector while  $\mathbf{p}$  denotes the two-vector transverse to the  $z$ -direction.

To include the local anisotropy in the plasma, one has to calculate the gluon polarization tensor incorporating anisotropic distribution functions of the medium. This subsequently can be used to construct HTL corrected gluon propagator which, in general, assumes very complicated form. Such an HTL propagator was first derived in [15] in time-axial gauge. Similar propagator has also been constructed in [16] to derive the heavy-quark potential in an anisotropic plasma, which, as we know, is given by the Fourier transform of the propagator in the static limit.

The self-energy, apart from momentum  $P^\mu$ , also depends on a fixed anisotropy vector  $n^\mu (= (1, \vec{n}))$  and  $\Pi^{\mu\nu}$  can be cast in a suitable tensorial basis appropriate for anisotropic plasma in a co-variant gauge in the following way [16]:

$$\Pi^{\mu\nu} = \alpha A^{\mu\nu} + \beta B^{\mu\nu} + \gamma C^{\mu\nu} + \delta D^{\mu\nu} \quad (4)$$

where the basis tensors are constructed out of  $p^\mu$ ,  $n^\mu$  and the 4-velocity of the heat bath  $u^\mu$ . The detailed expressions for the quantities those appear in Eq.(4) can be found in Ref. [15, 16]. The anisotropy enters through the distribution function given earlier (see Eq.(2)).

Since the self-energy is symmetric and transverse, all the components are not independent. After change of variables ( $p' = \vec{p}^2 [1 + \xi(\hat{\mathbf{p}} \cdot \vec{n})^2]$ ) the spatial components can be written as

$$\Pi^{ij} = \mu^2 \int \frac{d\Omega}{4\pi} v^i \frac{v^j + \xi(\vec{v} \cdot \vec{n})n^j}{1 + \xi(\vec{v} \cdot \vec{n})^2} \left( \delta^{ij} + \frac{v^j p^i}{P \cdot v + i\epsilon} \right) \quad (5)$$

Now  $\alpha, \beta, \gamma$  and  $\delta$  are determined by the following contractions:

$$\begin{aligned} p^i \Pi^{ij} p^j &= \vec{p}^2 \beta \\ A^{il} n^l \Pi^{ij} p^j &= (\vec{p}^2 - (n \cdot P)^2) \delta \\ A^{il} n^l \Pi^{ij} A^{jk} n^k &= \frac{\vec{p}^2 - (n \cdot P)^2}{\vec{p}^2} (\alpha + \gamma) \\ \text{Tr} \Pi^{ij} &= 2\alpha + \beta + \gamma \end{aligned} \quad (6)$$

where the expressions for  $\alpha, \beta, \gamma$  and  $\delta$  are given in Ref. [15].

After knowing the gluon HTL self-energy in anisotropic media the propagator can be calculated after some cumbersome algebra [16, 17]:

$$\begin{aligned} \Delta^{\mu\nu} &= \frac{1}{(P^2 - \alpha)} [A^{\mu\nu} - C^{\mu\nu}] \\ &+ \Delta_G \left[ (P^2 - \alpha - \gamma) \frac{\omega^4}{P^4} B^{\mu\nu} + (\omega^2 - \beta) C^{\mu\nu} + \delta \frac{\omega^2}{P^2} D^{\mu\nu} \right] - \frac{\lambda}{P^4} P^\mu P^\nu \end{aligned} \quad (7)$$

where

$$\Delta_G^{-1} = (P^2 - \alpha - \gamma)(\omega^2 - \beta) - \delta^2[P^2 - (n \cdot P)^2] \quad (8)$$

It is well known that the momentum space potential can be obtained from the static gluon propagator in the following way:

$$\begin{aligned} v(\mathbf{q}, \xi) \equiv v(\mathbf{q}, q_z = 0, \xi) &= g^2 \Delta^{00}(\omega = 0, \mathbf{q}, q_z = 0, \xi) \\ &= g^2 \frac{\vec{q}^2 + m_\alpha^2 + m_\gamma^2}{(\vec{q}^2 + m_\alpha^2 + m_\gamma^2)(\vec{q}^2 + m_\beta^2) - m_\delta^4} \end{aligned} \quad (9)$$

where, in general, the expressions for  $m_\alpha^2, m_\beta^2, m_\gamma^2$  and  $m_\delta^2$  are lengthy [16]. For  $q_z = 0$  (which is the case here) these simplify to [10]

$$\begin{aligned} m_\alpha^2 &= 0 \\ m_\beta^2 &= \mu^2 R(\xi) \\ m_\gamma^2 &= -\mu^2 \left[ \frac{1}{1 + \xi} - R(\xi) \right] \\ m_\delta^2 &= 0 \end{aligned} \quad (10)$$

for a parton propagating in the anisotropy direction. Here  $\mu$  is the Debye mass given by  $\mu^2 = g^2 p_{\text{hard}}^2 (1 + N_F/6)$ , where  $N_F$  is the number of flavours. In such case the two-body potential in anisotropic media simplifies to [10]

$$v(\mathbf{q}, \xi) = \frac{4\pi\alpha_s}{\mathbf{q}^2 + R(\xi)\mu^2} \quad (11)$$

with

$$R(\xi) = \frac{1}{2} \left[ \frac{1}{1 + \xi} + \frac{\tan^{-1} \sqrt{\xi}}{\sqrt{\xi}} \right] \quad (12)$$

Now the parton scatters with one of the colour centre with the momentum  $Q = (0, \mathbf{q}, q_z)$  and radiates a gluon with momentum  $K = (\omega, \mathbf{k}, k_z)$ . The method for calculating the amplitudes is discussed in Refs. [18, 19, 20] and we shall, for the sake of brevity, quote the main results only. The quark energy loss is calculated by folding the rate of gluon radiation ( $\Gamma(E)$ ) with the gluon energy by assuming  $\omega + q_0 \approx \omega$ . In this approximation one finds [18],

$$\frac{dE}{dL} = \frac{E}{D_R} \int x dx \frac{d\Gamma}{dx} \quad (13)$$

Here  $D_R$  is defined as  $[t_a, t_c][t_c, t_a] = C_2(G)C_R D_R$ , where  $C_2(G) = 3$ ,  $D_R = 3$  and  $[t_a, t_c]$  is a color commutator (see [18] for details).  $x$  is the longitudinal momentum fraction of the quark carried away by the emitted gluon.

Now in anisotropic media we have [10],

$$x \frac{d\Gamma}{dx} = \frac{C_R \alpha_s L}{\pi \lambda} \int \frac{d^2 \mathbf{k}}{\pi} \frac{d^2 \mathbf{q}}{\pi} |v(\mathbf{q}, \xi)|^2 \frac{\mu^2}{16\pi^2 \alpha_s^2} \left[ \frac{\mathbf{k} + \mathbf{q}}{(\mathbf{k} + \mathbf{q})^2 + \chi^2} - \frac{\mathbf{k}}{\mathbf{k}^2 + \chi} \right]^2 \quad (14)$$

In the last expression,  $v(\mathbf{q}, \xi)$  is the two body quark-quark potential given by Eq.(11) and  $\chi = m_q^2 x^2 + m_g^2$ , where  $m_g^2 = \mu^2/2$  and  $m_q^2 = \mu^2/6$ .

For arbitrary  $\xi$  the radiative energy loss can be written as [10]

$$\begin{aligned} \frac{\Delta E}{E} = & \frac{C_R \alpha_s L}{\pi^2 \lambda} \int dx d^2 \mathbf{q} \left[ \frac{\mu^2}{(\mathbf{q}^2 + R(\xi) \mu^2)^2} \left[ -\frac{1}{2} \right. \right. \\ & - \frac{k_m^2}{k_m^2 + \chi} + \frac{\mathbf{q}^2 - k_m^2 + \chi}{2 \sqrt{\mathbf{q}^4 + 2 \mathbf{q}^2 (\chi - k_m^2) + (k_m^2 + \chi)^2}} + \\ & \left. \left. \frac{\mathbf{q}^2 + 2\chi}{\mathbf{q}^2 \sqrt{1 + \frac{4\chi}{\mathbf{q}^2}}} \ln \left( \frac{k_m^2 + \chi}{\chi} \frac{(\mathbf{q}^2 + 3\chi) + \sqrt{1 + \frac{4\chi}{\mathbf{q}^2}} (\mathbf{q}^2 + \chi)}{(\mathbf{q}^2 - k_m^2 + 3\chi) + \sqrt{1 + \frac{4\chi}{\mathbf{q}^2}} \sqrt{\mathbf{q}^4 + 2 \mathbf{q}^2 (\chi - k_m^2) + (k_m^2 + \chi)^2}} \right) \right] \right] \end{aligned} \quad (15)$$

In the above expression,  $\lambda$  denotes the average mean free path of the quark given by

$$\frac{1}{\lambda} = \frac{1}{\lambda_g} + \frac{1}{\lambda_q} \quad (16)$$

which in this case would be  $\xi$  dependent. Note that  $\lambda_g$  and  $\lambda_q$  correspond to the contributions to the mean free path of the propagating quark coming from  $q$ - $g$  and  $q$ - $q$  scatterings.

Explicitly with Eq.(11) we have,

$$\lambda_i^{-1} = \frac{C_R C_2(i) \rho_i}{d_A} \int d^2 \mathbf{q} \frac{4 \alpha_s^2}{(\mathbf{q}^2 + R(\xi) \mu^2)^2}. \quad (17)$$

where  $C_R = 4/3$ ,  $C_2(i)$  is the cashimir for  $d_i$ -dimensional representation and  $C_2(i) = (N_c^2 - 1)/(2N_c)$  for quark and  $C_2(i) = N_c$  for gluon scatterers.  $d_A = N_c^2 - 1$  is the dimensionality of the adjoint representation and  $\rho_i$  is the density of the scatterers. Using  $\rho_i = \rho_i^{\text{iso}} / \sqrt{1 + \xi}$  we obtain

$$\frac{1}{\lambda} = \frac{18 \alpha_s p_{\text{hard}} \zeta(3)}{\pi^2 \sqrt{1 + \xi}} \frac{1}{R(\xi)} \frac{1 + N_F/6}{1 + N_F/4} \quad (18)$$

For  $\xi \rightarrow 0$  Eq.(18) reduces to well-known results [18]

$$\frac{1}{\lambda} = \frac{18 \alpha_s T \zeta(3)}{\pi^2} \frac{1 + N_F/6}{1 + N_F/4} \quad (19)$$

## 2.2 Hadronic $p_T$ spectrum

The high  $p_T$  inclusive hadron spectrum in a heavy ion collision can be calculated in a pQCD-improved parton model. There are various approaches about how to incorporate the energy loss in the hadron production from jet fragmentation. The differential cross-section for hadron production is [21],

$$\begin{aligned} E \frac{d\sigma}{d^3 p} (AB \rightarrow \text{jet} + X) = & K \sum_{abcd} \int dx_a dx_b G_{a/h_A}(x_a, Q^2) G_{b/h_B}(x_b, Q^2) \\ & \times \frac{\hat{s}}{\pi} \frac{d\sigma}{d\hat{t}} (ab \rightarrow cd) \delta(s + \hat{t} + u), \end{aligned} \quad (20)$$

Expressing the argument of the  $\delta$ -function in terms of  $x_a$  and  $x_b$  and doing the  $x_b$  integration we arrive at the final expression:

$$\begin{aligned} E \frac{d\sigma}{d^3p}(AB \rightarrow \text{jet} + X) &= K \sum_{abcd} \int_{x_{\text{amin}}}^1 dx_a G_{a/h_A}(x_a, Q^2) G_{b/h_B}(x_b, Q^2) \\ &\times \frac{2}{\pi} \frac{x_a x_b}{2x_a - x_T e^y} \frac{d\sigma}{dt}(ab \rightarrow cd) \end{aligned} \quad (21)$$

where  $x_b = (x_a x_T e^{-y})/(2x_a - x_T e^y)$ ,  $x_T = 2p_T/\sqrt{s}$  and  $x_{\text{amin}} = (x_T e^y)/(2 - x_T e^{-y})$ . It should be noted that to obtain single particle inclusive invariant cross-section in hadron-hadron collisions, the fragmentation function  $D_{h/c}(z, Q^2)$  must be included. Multiplying the result by the nuclear overlap function for a given centrality one can obtain the  $p_T$  distribution of hadrons in  $A-A$  collisions. However, the inclusion of jet-quenching as a final state effect in nucleus-nucleus collisions, can be implemented in two ways: (i) modifying the fragmentation function [22] and (ii) modifying the partonic  $p_T$  spectra [23] but keeping the fragmentation function unchanged. We shall concentrate on the former approach, as it is easier to include the final state effect in presence of anisotropy. Now the energy loss of high energy quarks and gluons traveling through dense colored plasma can measure the integrated density of the colored particles. This non-Abelian energy loss is a function of parton opacity  $L/\lambda$ . We use the expression given by Eq.(15) which is derived to first order in opacity.

Now in order to obtain the hadronic  $p_T$  spectrum in  $A-A$  collisions we modify the fragmentation function to obtain an effective fragmentation function as follows:

$$D_{h/c}(z, Q^2) = \frac{z^*}{z} D_{h/c}(z^*, Q^2) \quad (22)$$

where,  $z^* = z/(1 - \Delta E/E)$  is the modified momentum fraction. Also in order to take into account the jet production geometry we assume that all the jets are not produced at the same point and the path length traversed by these partons before fragmentation are not the same. It is also assumed that the jet initially produced at  $(r, \phi)$  leaves the plasma after a proper time ( $t_L$ ) or equivalently after traversing a distance  $L$  (for light quarks  $t_L \sim L$ ) given by  $L(r, \phi) = \sqrt{R_T^2 - r^2 \sin^2 \phi} - R_T \cos \phi$ , where  $R_T$  is the transverse dimension of the system. Now the hadron  $p_T$  spectra depends on the path length the initial parton must travel and the temperature profile along that path. As mentioned this is not the same for the all jets as it depends on the location where the jet is produced. Therefore we have to convolute the resulting expression over all transverse positions. Since the number of jets produced at  $\vec{r}$  is proportional to the number of binary collisions, the probability is proportional to the product of thickness functions :

$$\mathcal{P}(\vec{r}) \propto T_A(\vec{r}) T_B(\vec{r}) \quad (23)$$

For a hard sphere  $\mathcal{P}(r)$  is given by

$$\mathcal{P}(r) = \frac{2}{\pi R_T^2} \left(1 - \frac{r^2}{R_T^2}\right) \theta(R_T - r) \quad (24)$$

where  $\int d^2r \mathcal{P}(r) = 1$ . Using all these and noting that the path length is not a measurable quantity we obtain the  $p_T$  spectra of hadrons as follows:

$$\begin{aligned} \frac{dN^{\pi^0(\eta)}}{d^2p_T dy} &= \sum_f \int d^2r \mathcal{P}(r) \int_{t_i}^{t_L} \frac{dt}{t_L - t_i} \int \frac{dz}{z^2} \\ &\times D_{\pi^0(\eta)/f}(z, Q^2)|_{z=p_T/p_T^f} E \frac{dN}{d^3p^f}, \end{aligned} \quad (25)$$

The quantity  $E \frac{dN}{d^3p^f}$  is the initial momentum distribution of jets and can be computed using LO-pQCD (see Eq.(21)). For the fragmentation function Eq.(22) has been used. We use the average value of distance traversed by the partons,  $\langle L \rangle$  given by

$$\langle L \rangle = \frac{\int_0^{R_T} r dr \int_0^{2\pi} L(\phi, r) T_{AA}(r, b=0) d\phi}{\int_0^{R_T} r dr \int_0^{2\pi} T_{AA}(r, b=0) d\phi} \quad (26)$$

where  $\langle L \rangle \sim 5.8(6.2) fm$  for RHIC (LHC). The nuclear modification factor,  $R_{AA}$  is defined as

$$R_{AA}(p_T) = \frac{\frac{dN_{AA}^{\pi^0(\eta)}}{d^2p_T dy}}{\left[ \frac{dN_{AA}^{\pi^0(\eta)}}{d^2p_T dy} \right]_0} \quad (27)$$

where the suffix ‘0’ in the denominator indicates that energy loss has not been considered while evaluating the expression.

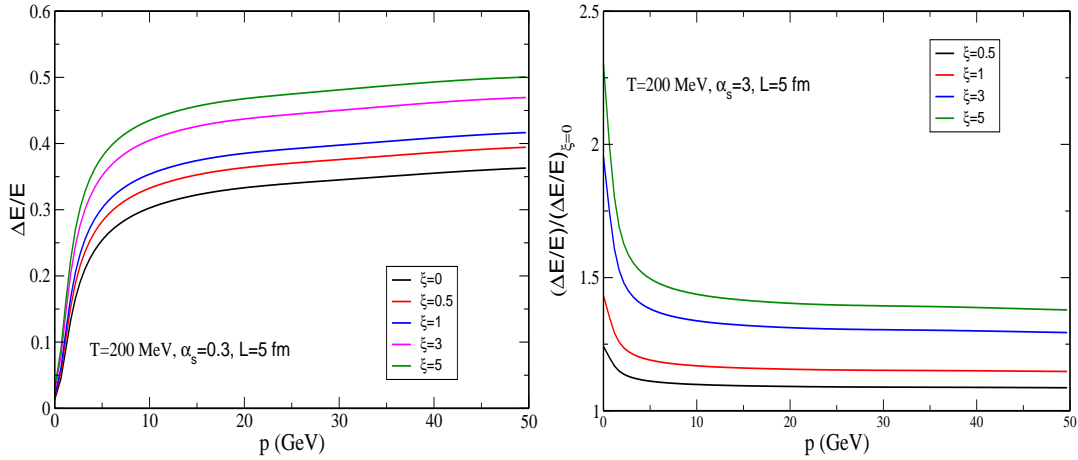


Figure 1: (Color online) Fractional energy loss for light quark when mean free path is independent of  $\xi$  (left panel). The ratio of the fractional energy loss of anisotropic media to that in isotropic media is also presented (right panel)



## 2.3 Space-time evolution

For an expanding plasma the anisotropy parameter  $\xi$  and the hard momentum scale  $p_{\text{hard}}$  (appearing in Eq.(15) via  $\lambda$  as well as in the expression of the Debye mass) are time dependent. Thus to calculate  $R_{\text{AA}}$  one needs to know the time dependence of  $p_{\text{hard}}$  and  $\xi$ . We shall follow the work of Ref. [24] to evaluate the  $p_T$  distribution of hadrons from the first few Fermi of the plasma evolution. Three scenarios of the space-time evolution (as described in Ref. [24]) are the following: (i)  $\tau_{\text{iso}} = \tau_i$ , the system evolves hydrodynamically so that  $\xi = 0$  and  $p_{\text{hard}}$  can be identified with the temperature ( $T$ ) of the system (till date all the calculations have been performed in this scenario), (ii)  $\tau_{\text{iso}} \rightarrow \infty$ , the system never comes to equilibrium, (iii)  $\tau_{\text{iso}} > \tau_i$  and  $\tau_{\text{iso}}$  is finite, one should devise a time evolution model for  $\xi$  and  $p_{\text{hard}}$  which smoothly interpolates between pre-equilibrium anisotropy and hydrodynamics. We shall follow scenario (iii) (see Ref. [24] for details) in which case the time dependence of the anisotropy parameter  $\xi$  is given by

$$\xi(\tau, \delta) = \left(\frac{\tau}{\tau_i}\right)^\delta - 1 \quad (28)$$

where the exponent  $\delta = 2$  ( $2/3$ ) corresponds to *free-streaming (collisionally-broadened)* pre-equilibrium momentum space anisotropy and  $\delta = 0$  corresponds to thermal equilibrium. As in Ref. [24], a transition width  $\gamma^{-1}$  is introduced to take into account the smooth transition from non-zero value of  $\delta$  to  $\delta = 0$  at  $\tau = \tau_{\text{iso}}$ . The time dependence of various quantities are, therefore, obtained in terms of a smeared step function [25]:

$$\Lambda(\tau) = \frac{1}{2}(\tanh[\gamma(\tau - \tau_{\text{iso}})/\tau_{\text{iso}}] + 1). \quad (29)$$

For  $\tau \ll \tau_{\text{iso}}$  ( $\gg \tau_{\text{iso}}$ ) we have  $\Lambda = 0(1)$  which corresponds to *free streaming* (hydrodynamics). With this, the time dependence of relevant quantities are as follows [24]:

$$\begin{aligned} \xi(\tau, \delta) &= \left(\frac{\tau}{\tau_i}\right)^{\delta(1-\Lambda(\tau))} - 1, \\ p_{\text{hard}}(\tau) &= T_i \bar{\mathcal{U}}^{c_s^2}(\tau), \end{aligned} \quad (30)$$

where,

$$\begin{aligned} \mathcal{U}(\tau) &\equiv \left[ \mathcal{R} \left( \left( \frac{\tau_{\text{iso}}}{\tau} \right)^\delta - 1 \right) \right]^{3\Lambda(\tau)/4} \left( \frac{\tau_{\text{iso}}}{\tau} \right)^{1-\delta(1-\Lambda(\tau))/2}, \\ \bar{\mathcal{U}} &\equiv \frac{\mathcal{U}(\tau)}{\mathcal{U}(\tau_i)}, \end{aligned} \quad (31)$$

$T_i$  is the initial temperature of the plasma and  $c_s^2$  is the velocity of sound. For isotropic case, we have  $p_{\text{hard}} = T$ ,  $\tau_{\text{iso}} = \tau_i$  so that  $\Lambda = 1$ ,  $\mathcal{U}(\tau) = \tau_i/\tau$ , and  $\mathcal{U}(\tau_i) = 1$ . By using  $c_s^2 = 1/3$  we recover the Bjorken cooling law [26]. We assume here that the plasma expands longitudinally as the effect of transverse expansion at the very early stage might be neglected. This has been illustrated in case of photon production in Ref. [27]. Since the momentum space anisotropy is an early stage phenomenon, this assumption is justified. Even if the

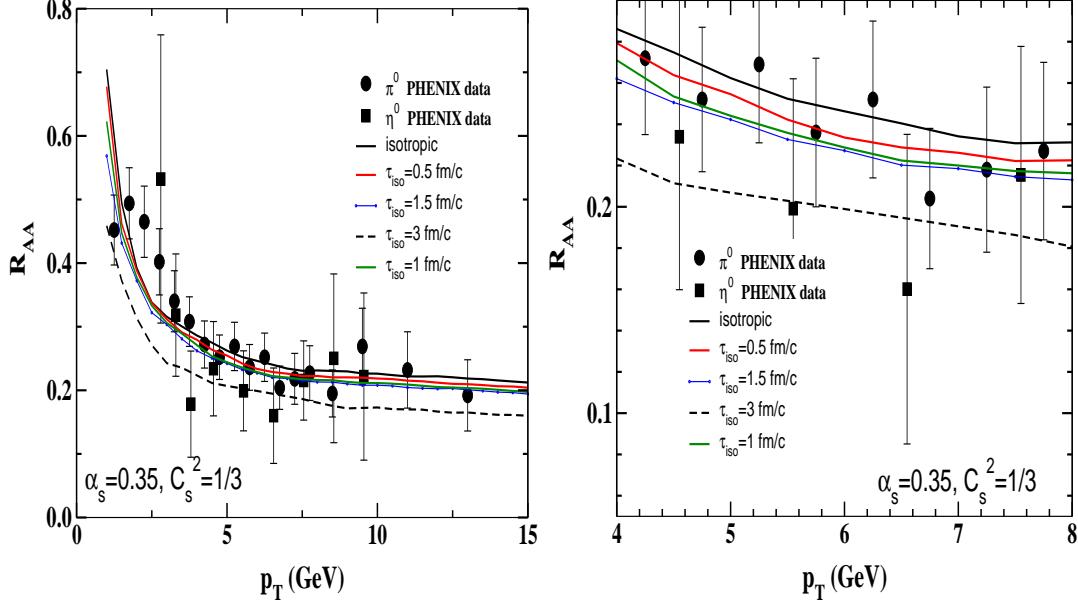


Figure 2: (Color Online) Nuclear modification factor at RHIC energies. The initial conditions are taken as  $T_i=440$  MeV and  $\tau_i=0.147$  fm/c. Left panel represents the results in the full  $p_T$  range whereas the in the right panel the results are given for  $4 \leq p_T \leq 8$  GeV

transverse expansion is important in the very early stage, it will have two effects on the parton energy loss : (i) The expanding geometry will increase the duration of propagation, and (ii) the same expansion will cause the parton density to fall along its path. These two effects partially compensate each other and the energy loss is almost the same as in the case without the transverse expansion [28].

Because the colliding nuclei do have a transverse density profile, we assume that the initial temperature profile is given by [29]

$$T_i(r) = T_i \left[ 2 \left( 1 - r^2/R_T^2 \right) \right]^{1/4} \quad (32)$$

Using Eqs.(30) and (32) we obtain the profile of the hard momentum scale as

$$p_{\text{hard}}(\tau, r) = T_i \left[ 2 \left( 1 - r^2/R_T^2 \right) \right]^{1/4} \bar{U}^{c_s^2}(\tau) \quad (33)$$

In the present work it is assumed that an isotropic QGP is formed at an initial temperature  $T_i$  and initial time  $\tau_i$ . Subsequent rapid longitudinal expansion leads to an anisotropic QGP which lasts till  $\tau_{\text{iso}}$ . Now in order to estimate the initial temperature we proceed as follows. In case of isentropic expansion the experimentally measured hadron multiplicity can be related to the initial temperature and thermalization time by the following equation [30]:

$$T_i^3(b_m)\tau_i = \frac{2\pi^4}{45\zeta(3)\pi R_T^2 4a_k} \left\langle \frac{dN}{dy}(b_m) \right\rangle \quad (34)$$

where  $\langle dN/dy(b_m) \rangle$  is the hadron (predominantly pions) multiplicity for a given centrality class with maximum impact parameter  $b_m$ ,  $R_T$  is the transverse dimension of the system,  $\tau_i$  is the initial thermalization time,  $\zeta(3)$  is the Riemann zeta function and  $a_k = (\pi^2/90) g_k$  is the degeneracy of the system created, where  $g_k = (7/8 \cdot 2 \cdot 2 \cdot N_F \cdot N_c + 2 \cdot 8)$ , and  $N_c$  being the number of colors. The hadron multiplicity resulting from  $Au + Au$  collisions is related to that from  $pp$  collision at a given impact parameter and collision energy by

$$\left\langle \frac{dN}{dy}(b_m) \right\rangle = \left[ (1-x) \langle N_{part}(b_m) \rangle / 2 + x \langle N_{coll}(b_m) \rangle \right] \frac{dN_{pp}}{dy} \quad (35)$$

where  $x$  is the fraction of hard collisions.  $\langle N_{part} \rangle$  is the average number of participants and  $\langle N_{coll} \rangle$  is the average number of collisions evaluated by using Glauber model.  $dN_{pp}^{ch}/dy = 2.5 - 0.25 \ln(s) + 0.023 \ln^2 s$  is the multiplicity of the produced hadrons in  $pp$  collisions at centre of mass energy,  $\sqrt{s}$  [31]. We have assumed that 20% hard (i.e.  $x = 0.20$ ) and 80% soft collisions are responsible for initial entropy production. This gives the desired multiplicity measured at RHIC energies. For 0 - 10% centrality (relevant for our case) we obtain  $T_i = 440$  (350) MeV for  $\tau_i = 0.147$  (0.24) fm/c.

We also calculate the nuclear modification factor at LHC energies at  $\sqrt{s} = 2.76$  TeV and  $\sqrt{s} = 5.5$  TeV. For the former case, the initial conditions are estimated as follows. The measured charged particle multiplicity density at this energy is [32]  $dN_{ch}/dy = 1600$  in most central collisions corresponding to  $\langle N_{part} \rangle \sim 382$  and  $\langle N_{coll} \rangle \sim 1700$  [33]. Using Eq.(34) we obtain  $T_i \sim 650$  MeV with  $\tau_i = 1$  fm/c. For LHC energies at  $\sqrt{s} = 5.5$ , the multiplicity in  $p-p$  collision is not known yet. We use the empirical formula for  $dN_{pp}/dy \sim 0.8 \ln \sqrt{s}$  which yields  $T_i = 830$  for  $\tau_i = 0.08$  fm/c.

### 3 Results

For the quantitative estimates of the fractional energy loss in an anisotropic media, we, first consider a plasma at a temperature  $T = 200$  MeV with effective number of degrees of freedom  $N_F = 2.5$  with the strong coupling as constant  $\alpha_s = 0.3$ . The fractional energy loss for non-zero  $\xi$  ( $\xi = 0.5, 1, 3, 5$ ) for light flavour is shown in Fig. (1) when the quark propagates along the direction of anisotropy. It is observed that as the anisotropy parameter ( $\xi$ ) increases, the fractional energy loss increases. The enhancement factor can be better understood by looking at the right panel of Fig. (1) where we have plotted the ratio of the fractional energy loss in anisotropic media to that in isotropic case. It is seen that at low momentum the enhancement is more and after that it saturates for all the values of  $\xi$  considered here. For larger values of the anisotropic parameter, the ratio is seen to increase reaching a maximum value of the order of 2 corresponding to  $\xi = 5$ . It is to be noted that the fractional energy loss decreases when the direction of propagation is not aligned with the anisotropy direction [10].

It is observed that the energy loss increases with the anisotropy parameter  $\xi$ . Mathematically, this can be understood as follows. The energy loss is proportional to the square of the two-body potential  $v(\mathbf{q}, \xi)$  which has a factor  $R(\xi)$  in the denominator. Now this quantity decreases with  $\xi$  and hence the fractional energy loss increases with  $\xi$ . It is also to be noted that the two-body potential is stronger when the parton propagates in the anisotropy direction and it decreases away from the anisotropy direction leading to less energy loss [10, 16, 34].

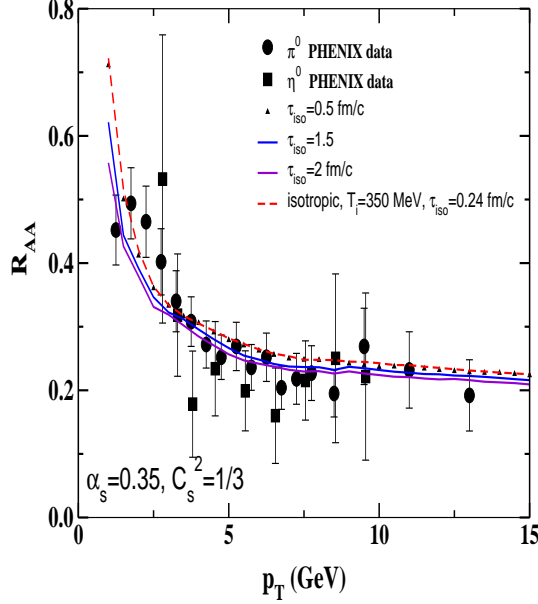


Figure 3: (Color Online) Same as Fig.(2) at  $T_i = 350$  MeV and  $\tau_i = 0.24$  fm/c.

Now let us turn to the calculation of nuclear modification factor at RHIC energies. For the time evolution of the system Eqs.(31) and (34) are used for free-streaming interpolating model ( $\delta = 2$ ). The initial conditions are taken as  $T_i = 440$  MeV and  $\tau_i = 0.147$  fm/c. The results for  $R_{AA}$  for various values of the isotropization time,  $\tau_{iso}$  have been compared with the PHENIX data [35] in Fig. (2). It is quite clear from right panel of Fig. (2) that the value of  $R_{AA}$  for anisotropic media is lower than that for the isotropic media as the energy loss in the former is higher by a factor of 1.2 - 2 (see Fig. (1)). It is also observed that as  $\tau_{iso}$  increases the value of  $R_{AA}$  decreases compared to its isotropic value. This is because the hard scale  $p_{hard}$  decreases slowly as compared to the isotropic case, i. e. the cooling is slow. Also we have checked that as  $\tau_{iso}$  increases the rate of cooling becomes slower leading to larger value of the energy loss. For reasonable choices of  $\tau_{iso}$ , the experimental data is well described. It is seen that increasing the value of  $\tau_{iso}$  beyond 1.5 fm/c grossly underpredict the data. We find that the extracted value of isotropization time lies in the range  $0.5 \leq \tau_{iso} \leq 1.5$  fm/c. This is in agreement with the earlier finding of  $\tau_{iso}$  using PHENIX photon data [36].

In order to see the sensitivity on the initial conditions we now consider another set of initial conditions,  $T_i = 350$  MeV and  $\tau_i = 0.24$  fm/c. The result is shown in Fig. (3). In this case also the data is well reproduced for the values of  $\tau_{iso}$  considered. It is observed that to reproduce the data larger value of  $\tau_{iso}$  is needed as compared to the case of higher initial temperature. We extract an upper limit of  $\tau_{iso} = 2$  fm/c in this case.

We also compare our results to the recent measurement of  $R_{AA}$  by the ALICE collaboration at  $\sqrt{s} = 2.76$  TeV [33]. The result is shown in Fig. (4). Note that LHC data, at this energy, show quite different behavior at high  $p_T$  (increasing trend) for which RHIC data do not exist. The reason might be due to larger volume and larger density. However, unlike the RHIC data, our present model is unable to explain the LHC data (only 2-3 points can

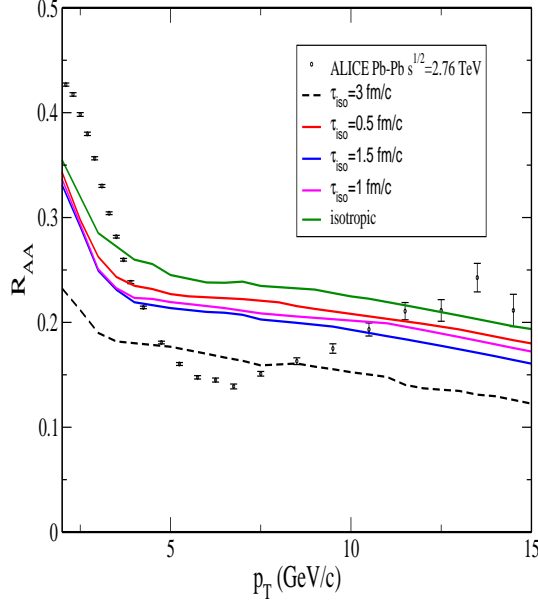


Figure 4: (Color Online) Same as Fig.(2) at  $\sqrt{s} = 2.76$  TeV corresponding to  $T_i = 650$  MeV and  $\tau_i = 0.1$  fm/c.

be explained with the values of  $\tau_{\text{iso}}$  considered here). Thus, within the ambit of the model used here, it is not possible to extract  $\tau_{\text{iso}}$  accurately at LHC energies. It is therefore, necessary to modify the present approach. The possible modifications might be the inclusions of collisional energy loss, path length distribution.

From the figures for  $R_{AA}$  (both for RHIC and LHC energies), it is observed that the nuclear modification factor shows some kind of saturation behavior with  $\tau_{\text{iso}}$ . We have checked that this occurs until  $\tau_{\text{iso}} = 1.5$  and 2 fm/c for two sets of initial conditions used at RHIC. Further increase of  $\tau_{\text{iso}}$  leads to more suppression thereby underpredicting the data (see Figs. (2)). Similar observations have been noted while calculating photons from anisotropic media [36].

Although for RHIC data we could extract  $\tau_{\text{iso}}$ , the extraction of  $\tau_{\text{iso}}$  is uncertain by comparing with the LHC data at  $\sqrt{s} = 2.76$  TeV. However, for the sake of completeness, we predict the nuclear modification factors at higher LHC energies, i. e. at  $\sqrt{s} = 5.5$  TeV. Since the final multiplicity at LHC energies is higher the initial temperature is higher compared to RHIC energies. Also the life time of the plasma is large. Moreover, the length traversed by the jets in the plasma is higher. As a result, one would expect that the energy loss would be more. Consequently,  $R_{AA}$  will be lower for the same values of isotropization time,  $\tau_{\text{iso}}$ . The results for various  $\tau_{\text{iso}}$  is delineated in Fig (5). As discussed earlier, we find that the values of the nuclear modification factors are less as compared to the case for RHIC.

So far we have used the interpolating models which assumes fixed initial conditions. However, enforcing fixed initial condition results in generation of particle number and enhance the final multiplicity during the transition from  $\delta = 2$  to zero. Because most of the experimental results correspond to fixed final multiplicity, we should device a mechanism which

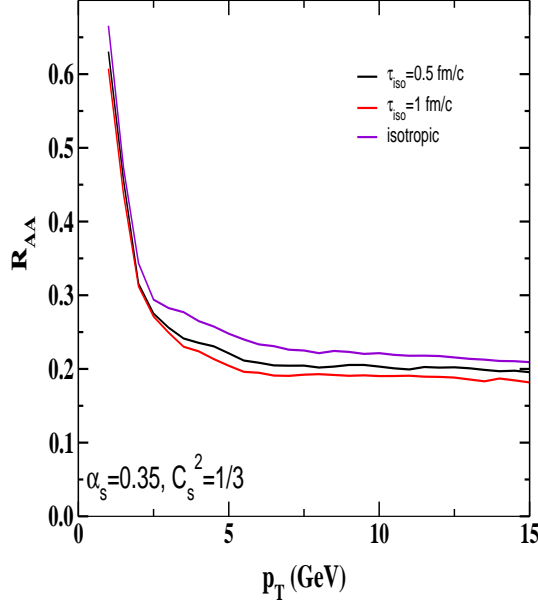


Figure 5: (Color Online) Same as Fig.(3) at LHC energies with  $T_i = 830$  MeV and  $\tau_i = 0.08$  fm/c.

enforces fixed final multiplicity. To do this the initial conditions have to be varied with the isotropization time, i. e. one must lower the initial "temperature" for finite  $\tau_{iso}$ . To ensure fixed final multiplicity in this model one has to redefine  $\bar{U}(\tau)$  in Eq. (31) as in [24]:

$$\bar{U}(\tau) = \mathcal{U}(\tau) \left[ \mathcal{R}((\tau_{iso}/\tau_i)^\delta - 1) \right]^{-3/4} (\tau_i/\tau_{iso})$$

This redefinition corresponds to a lower initial hard momentum scale ( $p_{hard}(\tau_i) < T_i$ ) for  $\tau_{iso} > \tau_i$ . Larger value of isotropization time corresponds to lower initial hard momentum scale. As we shall see, this has important consequences on the values of  $R_{AA}$ .

The result for fixed final multiplicity condition at RHIC energies has been displayed in Fig.(6). It is observed that the value of  $R_{AA}$  increases with  $\tau_{iso}$  compared to the isotropic case. The reason for this is that in FFM the larger the value of  $\tau_{iso}$  is, the lower is the initial hard momentum scale resulting less energy loss. This gives rise to higher value of  $R_{AA}$  as compared to the fixed initial condition (FIC) case as well as isotropic case. It is also seen that for FFM isotropic value of the nuclear modification factor is closer to the data in contrast to the observation made in case of FIC where it is possible to extract the value of the isotropization time at least for RHIC energies. Thus, use of FFM does not lead to any firm conclusion about the extraction of  $\tau_{iso}$ . We have checked that increasing the value of  $\tau_{iso}$  beyond 1.5 fm/c  $R_{AA}$  increases grossly underpredicting the data.

We reperform our calculation corresponding to Fig.(3) for FFM and the result is shown in Fig.(7). Similar behaviour (as in Fig.(6)) is observed for the reason mentioned above. Similarly, the calculations at LHC energies can be performed using FFM model. It is easy to guess that  $R_{AA}$  will be larger as compared to the case with FIC model.

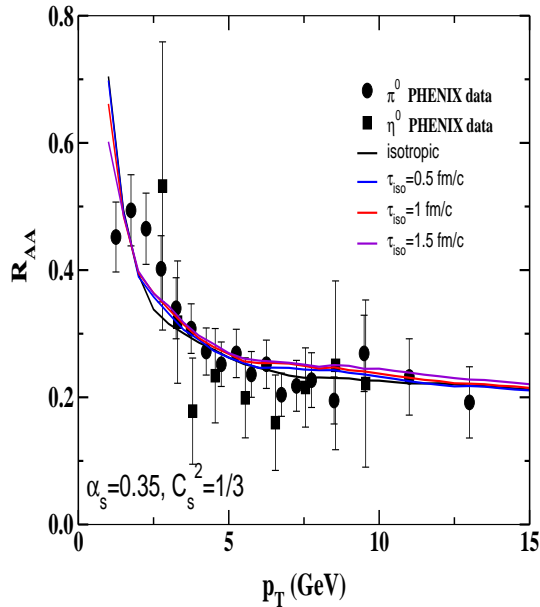


Figure 6: (Color Online) Same as Fig.(2) for fixed final multiplicity.

## 4 Summary

In this work, we have calculated the fractional energy loss due to gluon radiation in an infinite size anisotropic media treating the scatterer as providing a screened coulomb-like potential. It is shown that the presence of initial state anisotropy increases the radiative energy loss by a factor of 1.2 - 2 depending upon the values of the anisotropy parameter  $\xi$  and the momentum of the jet when the parton propagates along the direction of anisotropy. We then calculate the hadron  $p_T$  spectrum including this effect. A phenomenological model for the space time evolution of the anisotropic media has been used to obtain the time dependence of the anisotropy parameter and the hard momentum scale. The results for the nuclear modification factor for various values of the isotropization time  $\tau_{\text{iso}}$  are then compared with the PHENIX data. It is found that for FIC the data is well reproduced if  $\tau_{\text{iso}}$  lies in the range  $0.5 \leq \tau_{\text{iso}} \leq 1.5$  fm/c which is in agreement with the previous findings. Increasing  $\tau_{\text{iso}}$  beyond this range seems to underpredict the data. However, for FFM due to the lowering of the initial hard momentum scale with  $\tau_{\text{iso}}$ ,  $R_{AA}$  increases as compared to the case when FIC is used. By comparing with the data it is concluded that it is very difficult to infer which phase (isotropic or anisotropic) is favourable.

To cover the uncertainties in the initial conditions we also consider another set of initial conditions corresponding to RHIC energies. It is observed that for lower initial temperature the upper limit of the extracted value of  $\tau_{\text{iso}}$  is slightly higher as compared to the case where larger value of initial temperature is used. It is well known that the velocity of sound greatly influences the expansion dynamics. It has been seen that the results are extremely sensitive to the velocity of sound.

After fixing the model parameters from RHIC data, we calculate the nuclear modification

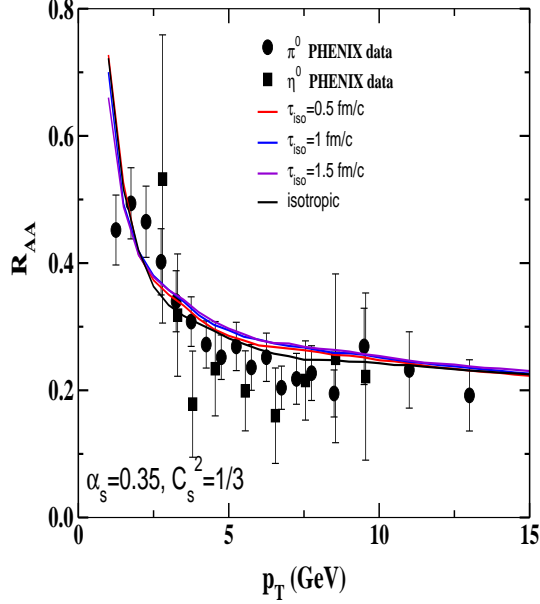


Figure 7: (Color Online) Same as Fig.(3) for fixed final multiplicity.

factor at LHC energies both at  $\sqrt{s} = 2.76$  and 5.5 TeV. The data at  $\sqrt{s} = 2.76$  is compared with our calculation. It is to be noted that the data at  $\sqrt{s} = 2.76$  show quite different behavior (decreasing between  $p_T = 5 - 10$  GeV and again increasing) than at RHIC energies. It is shown that the present model is unable to predict the isotropization time at these energies. In order to do that further refinement of the model is necessary. Note that as the initial temperature is higher, the nuclear modification factors are lower as compared to the RHIC case for the same set of parameters.

It is to be noted that we have not included the collisional energy loss in the present work as its contribution will be subleading. However, a complete calculation must include both the energy loss mechanisms in order to estimate  $\tau_{\text{iso}}$  i. e. better constrain can be imposed on  $\tau_{\text{iso}}$  in such case.

It is worthwhile to mention that the path length fluctuation is an important phenomenon as shown in Ref. [37] while explaining the non-photon single electron data. In addition to the anisotropy parameter  $\xi$ , the energy loss of parton in anisotropic media also depends on the direction of propagation with respect to the anisotropy axis. Therefore, consideration of fluctuating path length might lead to additional direction dependence. In addition, use of path length distribution (instead of constant value) leads to surface emission effects which plays significant role in determining  $R_{AA}$ .

It is to be mentioned that we have used the average energy loss to calculate the nuclear modification factor. However, to improve our calculation statistical treatment of the energy loss has to be incorporated. In our calculation of energy loss Landau-Pomeranchuk effect has been neglected which is worth investigating.

We also do not consider the recoil of the scatterer in this work. However, this condition can be relaxed by incorporating the recoil corrections which plays an important role as shown



in Ref. [18]. Also this will lead to the unstable modes which greatly influences the transport coefficients, such as the radiative energy loss. This will be included in future publication. Furthermore, the finite size effect to the radiative energy loss in anisotropic media would also be interesting to study. We leave these issues for now.

## References

- [1] J. D. Bjorken, Fermilab-Pub-82/59-THY(1982) and Erratum (Unpublished).
- [2] J. D. Bjorken, Fermilab-Pub-82/59-THY(1982) and Erratum (Unpublished); M. Gyulassy, P. Levai and I. Vitev, Nucl. Phys. B **571**, 197 (2000); B. G. Zakharov, JETP Lett. **73**, 49 (2001); M. Djordjevic and U. Heinz, Phys. Rev. Lett **101**, 022302 (2008); R. Baier *et al.*, J. High Ener. Phys. **0109**, 033 (2001); S. Jeon and G. D. Moore, Phys. Rev. **C71**, 034901 (2005); A. K. Dutt-Mazumder, J. Alam, P. Roy, and B. Sinha, Phys. Rev. D **71**, 094016 (2005); P. Roy, J. Alam, and A. K. Dutt-Mazumder, J. Phys. G. **35**, 104047 (2008).
- [3] U. W. Heinz, arXiv:nucl-th/0512051.
- [4] R. Baier, A. H. Muller, D. Schiff and D. T. Son, Phys. Lett. **B502**, 51 (2001).
- [5] M. Luzum and P. Romatschke, Phys. Rev. C **78**, 034915 (2009).
- [6] S. Mrowczynski, Phys. Lett. **B314** 118 (1993); S. Mrowczynski, Acta. Phys. Pol. B **37**, 427 (2006); P. Arnold, J. Lenghan, G. D. Moore and L. G. Yaffe, Phys. Rev. Lett. **94**, 072302 (2005); A. Rebhan, P. Romatschke and M. Strickland, Phys. Rev. Lett. **94**, 102303 (2005); P. Romatschke and R. venugopalan, Phys. Rev. Lett **96**, 062302. (2006)
- [7] W. Jas and S. Mrowczynski, Phys. Rev. C **76**, 044905 (2007).
- [8] P. Romatschke and M. Strickland, Phys. Rev. D **71**, 125008 (2005).
- [9] P. Romatschke and M. Strickland, Phys. Rev. D **69**, 065005 (2005).
- [10] P. Roy and A. K. Dutt-Mazumder, e-Print: arXiv:1009.2304
- [11] A. Majumder, B. Muller, and St. Mrowczynski, Phys. Rev. **D80**, 125020 (2009).
- [12] M. Gyulassy and X. N. Wang, Nucl. Phys. **B420**, 583 (1994).
- [13] M. Asakawa, S. A. Bass, and B. Muller, Prog. Theor. Phys. **116**, 725 (2007).
- [14] J. P. Blaizot and E. Iancu, Phys. Rep. **359**, 355 (2002).
- [15] P. Romatschke and M. Strickland, Phys. Rev. **D68**, 036004 (2005).
- [16] A. Dumitru, Y. Guo, and M. Strickland, Phys. Lett. **B662**, 37 (2008).
- [17] R. Baier and Y. Mehtar-Tani, Phys. Rev. **C78**, 064906 2008.

- [18] M. Djordjevic, Phys. Rev. **C80**, 064909 (2009)
- [19] M. Djordjevic and M. Gyulassy, Phys. Lett. **B560**, 37 (2003)
- [20] M. Djordjevic and M. Gyulassy, Nucl. Phys. **A733**, 265 (2004)
- [21] J. F. Owens, Rev. Mod. Phys. **59**, 465 (1987).
- [22] X. N. Wang, Phys. Rev. C **58**, 2321 (1998).
- [23] P. Roy, A. K. Dutt-Mazumder and J. Alam, Phys. Rev. C **73**, 044911 (2006).
- [24] M. Martinez and M. Strickland, Phys. Rev. C **78**, 034917 (2008).
- [25] M. Martinez and M. Strickland, Phys. Rev. Lett. **100**, 10231 (2008).
- [26] J. D. Bjorken, Phys. Rev. D **27**, 140 (1983).
- [27] T. Renk, Phys. Rev. C **71**, 064905 (2005).
- [28] M. Gyulassy, I. Vitev, X. N. Wang, and P. Huovinen, Phys. Lett. **B526**, 301 (2002).
- [29] S. turbide, C. Gale, S. Jeon, and G. D. Moore , Phys. Rev. C **72**, 014906 (2005).
- [30] R. C. Hwa R C and K. Kajantie, Phys. Rev. D **32**, 1109 (1985).
- [31] D. Khazreev and M. Nardi, Phys. Lett. **B507**, 121 (2001)
- [32] K. Aamodt et al, ALICE Collaboration, Phys. Rev. Lett. **106**, 032301 (2011); Aamodt et al, ALICE Collaboration, Phys. Rev. Lett. **105**, 252301 (2011).
- [33] K. Aamodt et al, ALICE Collaboration, Phys. Lett. **B690**, 30 (2011).
- [34] A. Dumitru, Y. Nara, B. Schenke, and M. Strickland, Phys. Rev. C **78**, 024909 (2008).
- [35] S. S. Adler *et al.*, PHENIX collaboration, Phys. Rev. Lett. **96** (2006) 202301.
- [36] L. Bhattacharya and P. Roy, Phys. Rev. C **79**, 054910 (2009).
- [37] S. Wicks, W. Horowitz, M. Djordjevic, and M. Gyulassy, Nucl. Phys. A **784**, 426 (2007).